

Comparison of the Rat Nucleolar Protein Nopp140 with Its Yeast Homolog SRP40

DIFFERENTIAL PHOSPHORYLATION IN VERTEBRATES AND YEAST*

(Received for publication, April 9, 1996, and in revised form, May 23, 1996)

U. Thomas Meier†

From the Department of Anatomy and Structural Biology, Albert Einstein College of Medicine, Bronx, New York 10461

Rat Nopp140, a nonribosomal protein of the nucleolus and coiled bodies, was characterized as one of the most highly phosphorylated proteins in the cell. Based on its subcellular location, its nuclear localization signal binding capacity, and its shuttling between the nucleolus and the cytoplasm, Nopp140 was proposed to function as a chaperone in ribosome biogenesis. This study shows that casein kinase II phosphorylates Nopp140 to its unusual high degree and identifies the yeast *SRP40* gene product as immunologically and structurally related to rat Nopp140. *SRP40* encodes an acidic (pI = 3.9), serine-rich (49%) protein of 41 kDa whose carboxyl terminus exhibits 59% sequence identity to that of Nopp140. *SRP40* localizes to the yeast nucleolus and is required at a specific cellular concentration for optimal growth as indicated by the negative effect on cell growth of both overexpression and deletion of its gene. Like Nopp140, *SRP40* is phosphorylated by casein kinase II, but to a much lesser extent. While the parallels between these two proteins suggest that *SRP40* is the bona fide yeast Nopp140 homolog, their disparities reflect the differences in nucleolar dynamics and regulation of ribosome biogenesis between yeast and vertebrates.

The nucleolus is the site of ribosomal RNA transcription and processing and of assembly of preribosomal particles. The latter requires import from the cytoplasm of ribosomal proteins and subsequent export of the preassembled ribosomes. While functional bacterial ribosomes can be assembled under non-physiological conditions *in vitro* (1), *in vivo*, cellular factors or chaperones are required for ribosome biogenesis. Several non-ribosomal proteins within the nucleolus have been identified that are candidates for such chaperones (for a recent review see Ref. 2).

Nonribosomal nucleolar proteins were identified over 20 years ago (3–5) and, like ribosomal proteins, are often evolutionarily conserved. This was illustrated recently by our identification of a rat liver nucleolar protein, NAP57, that exhibits sequence similarity to yeast (71% sequence identity with yeast CBF5; Ref. 6) and prokaryotic proteins (7). Indeed, most vertebrate nucleolar proteins reveal homology, on various levels, with yeast proteins. Some examples include mammalian fibrillar (8), which is immunologically, structurally, and function-

ally related to yeast NOP1 (9, 10), human p120 (11), which is 67% identical to yeast NOP2 over approximately half its protein sequence (12), and mammalian nucleolin/C23 (3, 13), which shows homology in its domain structure to yeast NSR1 (14–16). The study of some of these yeast homologs has revealed their involvement in rRNA processing and/or ribosome assembly, *e.g.* NOP1 (17), and led to the discovery of additional nonribosomal nucleolar proteins, *e.g.* GAR1 (18), SOF1 (19), and NOP77/NOP4 (20, 21).

Nucleolar proteins contain a variety of characteristic domains, such as RNA recognition motifs and glycine/arginine-rich repeats, both for association with RNA, and acidic stretches apparently for interaction with basic ribosomal proteins. The most unusual of the nucleolar proteins with an acidic stretch is Nopp140 (22). Its central domain harbors 10 repeats consisting of runs of 13–17 consecutive serine, aspartic, and glutamic acid residues separated by exclusively basic stretches of 23–46 residues rich in lysine, alanine, and proline. We originally identified Nopp140 as a nuclear localization signal binding protein in the nucleolus of rat liver (23) and subsequently also localized it to coiled bodies (7). It is one of the most highly phosphorylated proteins in the cell with up to 82 mol of phosphate/molecule (22). The phosphorylation apparently occurs in the acidic serine repeats and leads to the dramatic drop from the theoretical isoelectric point of 10.3 to 4.1. While located mostly in the nucleolus, Nopp140 constantly shuttles between the nucleolus and the cytoplasm on nucleoplasmic tracks (22). In addition, Nopp140 exists in a stoichiometric complex with the highly conserved protein NAP57 (see above; Ref. 7). We have proposed Nopp140, based on its nucleolar location, shuttling, nuclear localization signal binding, and acidic serine repeats, to function as a chaperone in ribosome assembly and/or nuclear transport of nucleolar components. Yet many questions regarding its function and mode of action remain. How does phosphorylation affect shuttling, and what is the kinase responsible for the enormous degree of phosphorylation? Is Nopp140 as highly conserved as its associated protein, NAP57, and can that be exploited to further define its function?

This study shows that casein kinase II (CKII)¹ phosphorylates Nopp140 to its unusual high degree and that this phosphorylation also occurs in yeast cells. Antibody cross-reactivity reveals the yeast *SRP40* gene product as immunologically related to rat Nopp140, and sequence comparison shows the two proteins to be structurally similar, with the carboxyl terminus exhibiting 59% sequence identity. While the *SRP40* gene has been identified in several genetic screens (24–26), its product, *SRP40*, remained uncharacterized. *SRP40* is an acidic (pI =

* This work was supported by National Institutes of Health Grant GM50725. The costs of publication of this article were defrayed in part by the payment of page charges. This article must therefore be hereby marked "advertisement" in accordance with 18 U.S.C. Section 1734 solely to indicate this fact.

† To whom correspondence should be addressed: Dept. of Anatomy and Structural Biology, Albert Einstein College of Medicine, 1300 Morris Park Ave., Bronx, NY 10461. Tel.: 718-430-3294; Fax: 718-430-8996; E-mail: meier@acom.yu.edu.

¹ The abbreviations used are: CKII, casein kinase II; BRL, buffalo rat liver; GST, glutathione *S*-transferase; HA, hemagglutinin; SC, synthetic complete; MOPS, 4-morpholinepropanesulfonic acid; PAGE, polyacrylamide gel electrophoresis; PCR, polymerase chain reaction.

3.9), serine-rich (49%) protein of 41 kDa that is localized to the nucleolus. It is required at a specific cellular concentration for optimal growth as indicated by the negative effect on growth of both overexpression and deletion of its gene. Bacterially expressed SRP40 is phosphorylated by CKII like Nopp140, but to a much lesser extent. These data are discussed in the context of the similarities and differences in the regulation of ribosome biogenesis and nucleolar dynamics between yeast and vertebrates.

EXPERIMENTAL PROCEDURES

DNA Constructs

All DNA manipulations were performed employing standard procedures (27) and as described previously (7, 22). The polymerase chain reaction (PCR) was routinely performed with the hot start technique to avoid false priming, and the newly generated linker sequences of the PCR products were confirmed by DNA sequencing. The *SRP40* DNA inserted in the constructs below was isolated by PCR amplification using yeast genomic DNA as template and primers that created the indicated restriction sites.

pET8c/Nopp140 (Nopp140 Bacterial Expression Vector)—The open reading frame of Nopp140 was amplified by PCR with primers, generating an *NcoI* site at the initiating methionine and a *BamHI* site 25 nucleotides downstream of the stop codon, using the original λ DNA (pTM17; Ref. 22) as template. The PCR product was cloned into the corresponding sites of the prokaryotic expression vector pET8c (28), and the resulting construct was transformed into BL21 (DE3) cells for expression.

pTM25 (Nopp140 Yeast GAL10, LEU2, CEN6, ARS4 Expression Vector)—The open reading frame of Nopp140 was amplified as described for the pET8c/Nopp140 construct with the exception that the 5'-primer added a *BamHI* instead of an *NcoI* site. The product was cloned into the *BamHI* site of pRS315G (a kind gift from Susan Smith; Ref. 29) such that the complete coding sequence of Nopp140 plus an extra amino-terminal serine and glycine were fused in frame to the second amino acid of the *CYC1* gene under control of the *GAL10* promoter.

pTM52 (GST-SRP40 Bacterial Expression Vector)—The coding region of the *SRP40* gene with a *NcoI* site at the initiating methionine and a *XhoI* site in place of the stop codon was cloned into those sites of pGEX-KG (a kind gift from Gang Liu; Ref. 30), creating a continuous open reading frame between glutathione *S*-transferase (GST) and *SRP40* with an additional eight codons after which a stop codon was provided by the vector in all three reading frames.

pTM50 (GST-SRP40C-term Bacterial Expression Vector)—The DNA encoding the conserved last 51 amino acids of *SRP40* with a 5'-*NcoI* site (encoding an in frame methionine) and a 3'-*XhoI* site in place of the stop codon was cloned into the pGEX-KG vector as described for pTM52.

pTM36 (SRP40-HA Yeast GAL1, URA3, 2 μ Expression Vector)—The coding region of *SRP40* with a 5' *EcoRI* site and a 3' *KpnI* site was cloned into those sites of pJD305 (Jürgen Dohmann, Heinrich Heine University, Düsseldorf, Germany; based on pLGS5, Ref. 31) in frame with a double carboxyl-terminal hemagglutinin (HA) epitope tag (32) generating pTM35. The SRP40-HA construct was excised from pTM35 with *EcoRI* and *XbaI* and cloned into those sites of pYES2 (Invitrogen, San Diego, CA) placing the SRP40-HA construct under the inducible control of the *GAL1* promoter.

pTM41 (HA-SRP40 Yeast GAL10, LEU2, CEN6, ARS4 Expression Vector)—The open reading frame of *SRP40* was subcloned into pC11,² generating an in frame amino-terminal HA epitope tag. The HA-SRP40 construct was further subcloned into the *SpeI* and *NotI* sites of pRS315G (29) in frame with the first five amino acids of the *CYC1* gene under the inducible control of the *GAL10* promoter.

pTM33 (Construct for SRP40 Gene Deletion)—The *SRP40* gene including 1020-nucleotide 5'- and 960-nucleotide 3'-untranslated region with a 5' *SaI* and a 3' *XbaI* site was cloned into the *XhoI* and *XbaI* sites of pBluescript II SK⁺ (Stratagene, La Jolla, CA) generating pTM32. The *URA3* gene, isolated by PCR amplification with pRS316 (33) as template, was inserted in reverse orientation into the *XhoI* and *EcoRI* sites of pTM32 while dropping out the entire *SRP40* coding region as shown schematically in Fig. 7A. The construct containing the *SRP40* 3'- and 5'-flanking region with the *URA3* gene inserted was excised from pTM33 using *XbaI* and *KpnI* and used directly to transform diploid yeast strains.

Yeast Strains and Cell Growth

All strains used in this study were derived from the diploid strains W303 (*Mata/Mata ade2-1/ade2-1 ura3-1/ura3-1 his3-11,15/his3-11,15 trp1-1/trp1-1 leu2-3,112/leu2-3,112 can1-100/can1-100*; kind gift from Amy Chang) and DF5 (*Mata/Mata ura3-52/ura3-52 his3- Δ 200/his3- Δ 200 trp1-1/trp1-1 leu2-3,112/leu2-3/112 lys2-801/lys2-801*; kind gift from John Aitchison). TMX14 corresponds to W303 with one copy of the *SRP40* gene replaced by the *URA3* gene (*srp40 Δ ::URA3*) and, analogously, TMX15 corresponds to DF5 (*srp40 Δ ::URA3*). F1104 is the haploid *Mata* strain isogenic with W303, while TMY20 corresponds to F1104 with the *SRP40* gene replaced by the *URA3* gene (*srp40 Δ ::URA3*). The following strains were generated by transformation of the indicated strains with respective plasmids (in parentheses) using the lithium acetate method (34) and selection on synthetic complete (SC) medium containing 2% glucose but lacking the corresponding marker (see respective plasmids); TMX12 = W303 (pTM25), TMX13 = W303 (pRS315G), TMX19 = W303 (pYES2), TMX23 = W303 (pTM36), TMX33 = W303 (pTM41), and TMY28 = F1104 (pTM41).

Expression of the genes encoded by the plasmids was induced from the *GAL* promoter by either growing the cells overnight in the presence of 2% galactose or by switching from 2% raffinose to 2% galactose containing SC medium lacking the corresponding markers for 90 min followed by suppression of the expression in rich medium (YPD; 1% yeast extract, 2% bactopeptone, 2% dextrose; Ref. 35) as described under "Results." No difference in localization of the induced gene products was observed between the two methods.

The strains deleted in one copy of the *SRP40* gene, TMX14 and TMX15, were created by homologous recombination through transformation of W303 and DF5, respectively, with the linearized pTM33 construct and selection for growth on SC medium lacking the uracil marker. The haploid strain TMY20 (*Mata srp40 Δ ::URA3*) was selected from the segregants that resulted from sporulation and subsequent tetrad dissection of TMX14 and that grew when replica-plated on SC medium lacking uracil (see Fig. 7, A–D). Proper genomic integration of the *URA3* gene and consequent deletion of the *SRP40* gene was confirmed in all strains by the production of the expected size products upon PCR amplification when using the corresponding genomic DNA as template combined with three primers, one outside the pTM33 construct and one each within the *URA3* and the *SRP40* gene (not shown).

Growth rates of F1104 and TMY20 were determined in liquid SC medium and, in the case of TMY28, in SC medium lacking leucine by diluting a freshly grown late stationary phase culture about 100-fold in fresh medium. Growth at 30 °C was observed by measuring the optical density at 600 nm. Yeast cell culture, genomic DNA preparation, total yeast extracts for SDS-PAGE, and general manipulations were performed essentially as described (36).

Production and Purification of Recombinant Proteins

E. coli BL21(DE3) cells (28) transformed with pET8c/Nopp140, pTM52, or pTM50 were grown in L-broth containing 100 μ g/ml ampicillin until $A_{600} = 0.8$ and expression of Nopp140 and the GST-SRP40 fusion proteins was induced by the addition of 1 mM isopropyl-1-thio- β -D-galactopyranoside and continued for 2 h at 37 °C. At this point, the cells were either lysed directly in SDS sample buffer for analysis of whole cell extracts or further processed for purification of the recombinant proteins.

Overexpressed Nopp140 was predominantly insoluble and segregated into inclusion bodies, which were isolated and washed as described (37). The inclusion bodies were solubilized in 6 M urea followed by a dropwise dilution (10-fold final) into 10 mM potassium phosphate buffer (pH 8.1) at room temperature. After stirring for an additional 30 min, the solubilized Nopp140 solution was cleared at 27,000 \times g for 30 min and loaded onto a hydroxylapatite (Bio-Gel HTP; Bio-Rad) column equilibrated with 10 mM potassium phosphate buffer (pH 8.1) at room temperature. The column was washed consecutively with equilibration buffer, 100 mM and 200 mM potassium phosphate buffer, and the homogeneous recombinant Nopp140 eluted with 300 mM and 400 mM phosphate buffer. Recombinant Nopp140 was subsequently dialyzed against phosphate-buffered saline and concentrated in Centricon 50 concentrators (Amicon, Inc., Beverly, MA).

About 20% of overexpressed GST-SRP40 was soluble in the 10 mM Tris (pH 8.0), 1 mM EDTA supernatant after the bacteria were lysed first by incubation with 10 μ g/ml lysozyme for 30 min at room temperature, second by one freeze-thaw cycle, third by the addition of 20 mM magnesium chloride, 5 μ g/ml DNase I (Sigma) (a protease inhibitor mixture previously used in the purification of Nopp140 (23)) and incubation at 37 °C for 15 min, and fourth by tip sonication on ice after the

² C. Isaac and U.T. Meier, unpublished results.

addition of 150 mM sodium chloride and 1% Triton X-100. The bacterial lysate was clarified by centrifugation at $47,000 \times g$ for 10 min at 4 °C and GST-SRP40 adsorbed onto glutathione-Sepharose 4B (Pharmacia Biotech Inc.) packed in a column and equilibrated with phosphate-buffered saline containing 1% Triton X-100. The column was washed consecutively with equilibration buffer; 10 mM Tris (pH 8.0), 1 M sodium chloride; and 50 mM Tris (pH 8.0); and purified recombinant GST-SRP40 was eluted with 10 mM glutathione in 50 mM Tris (pH 8.0). GST-SRP40 was concentrated and free glutathione was removed by two cycles of concentration and dilution into 10 mM Tris, pH 8.0, in Centri-con-50 concentrators (Amicon).

Immunochemical Methods

Polyclonal antibodies were raised in rabbits against the purified recombinant Nopp140 essentially as described (23) by Rockland Inc. (Gilbertville, PA). Western blots were performed as described previously (23) with the exception that enhanced chemiluminescence (ECL, Amersham Corp.) was used to detect the antibodies according to the specifications of the manufacturer. Primary antibodies on immunoblots were used at the following dilutions: antirecombinant Nopp140 antiserum at 1:1000, affinity-purified anti-Nopp140 peptide IgGs (22) at 0.2 μ g/ml, anti-pp135 antiserum (kindly provided by Alfred Anderer; Ref. 38) at 1:500, and 12CA5 anti-HA ascites fluid (kindly provided by Jonathan Backer and directed against the HA peptide YPYDCPDYA; Ref. 32) at 1:5000.

Indirect immunofluorescence on buffalo rat liver (BRL) cells was done essentially as described (23) using the antirecombinant Nopp140 antiserum at a dilution of 1:1000 in phosphate-buffered saline containing 2% bovine serum albumin. Yeast cells were prepared for indirect immunofluorescence essentially as described (39). Briefly, cells growing in log phase were fixed for 5 min with 3.7% formaldehyde, spheroplasts were prepared by a 1.5-h incubation with glucuronidase (diluted 1:10; DuPont) and zymolyase 100T (100 μ g/ml; ICN Immunochemicals, Costa Mesa, CA) at 30 °C, and the spheroplasts were attached onto polylysine-coated coverslips and permeabilized in cold methanol and acetone. Antibodies were incubated in phosphate-buffered saline containing 2% bovine serum albumin at the following dilutions: antirecombinant Nopp140 antiserum at 1:50, anti-Nopp140 peptide IgGs (22) at 1 μ g/ml, anti-HA ascites fluid at 1:100, and A66 anti-Nop1 monoclonal antibody ascites fluid (kindly provided by John Aris; Ref. 40) at 1:100. DNA was stained with propidium iodide (20 μ g/ml), and secondary antibodies were applied for double fluorescence as described previously (7). Fluorescence was observed on two wavelengths simultaneously using an MRC-600 laser-scanning confocal microscope (Bio-Rad). The pictures were processed on a Macintosh computer using NIH Image and Adobe Photoshop software and directly printed on a Kodak Colorex printer, as were the images of the gels and autoradiograms after digitization on a flatbed scanner with transparency adaptor (Hewlett Packard ScanJet IICx).

Phosphorylation

Recombinant Nopp140 and GST-SRP40, 0.5 μ g each, were incubated for 1 h at 37 °C in the presence or absence of 16 ng of purified sea star CKII (Upstate Biotechnology Inc., Lake Placid, NY) in 50 mM MOPS buffer (pH 7.0) containing 50 mM sodium chloride, 5 mM magnesium chloride, 5 mM EGTA, and 1 mM each ATP and GTP (10 μ l total volume). The reaction was stopped by the addition of 10 μ l of double-concentrated sample buffer and analyzed by SDS-PAGE and Coomassie Blue or silver stain as described (7). When [γ - 32 P]-ATP (10 μ Ci/sample, Amersham Corp.) was used in phosphorylation assays, only half the amounts of substrates and CKII were added, and the dried SDS-PAGE gels were exposed for autoradiography to Kodak XAR film for an average of 1 min.

Protein analyses, such as isoelectric point calculations and sequence alignments, were performed using the GeneWorks software package (IntelliGenetics, Inc., Mountain View, CA). The pK values for phosphoserine were approximated from those of phosphocarbon esters (41), which resulted in calculated isoelectric points close to those experimentally determined, *i.e.* pI for *Xenopus* Nopp140 (42) = 4.0 (theoretical) and 4.2 (experimental; Ref. 43). GenBank™ searches were performed by the BLAST algorithm (44).

RESULTS

Nopp140 Is an Extreme Substrate for Casein Kinase II—One of the hallmarks of Nopp140 is its high degree of phosphorylation and its mobility shift on SDS-PAGE from M_r 140 to M_r 100 upon phosphatase treatment (22). Nopp140 contains 49

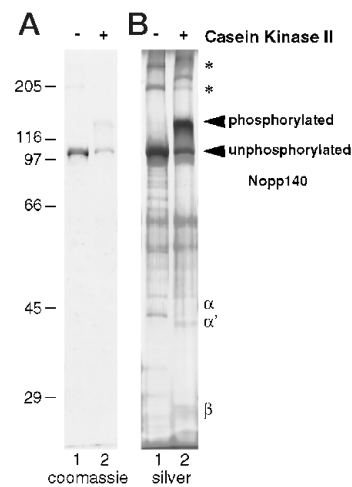


FIG. 1. CKII phosphorylates recombinant Nopp140 *in vitro*. Recombinant Nopp140 (0.5 μ g) was incubated in the absence (lanes 1) and presence (lanes 2) of 30-fold less purified sea star CKII and analyzed on SDS-PAGE by Coomassie Blue (A) and subsequent silver stain (B). Note the enormous mobility upshift and enhanced silver stainability upon CKII phosphorylation (arrowheads). Asterisks indicate the mobility of putative dimeric and trimeric forms of Nopp140, which upshift as well upon phosphorylation. The migrating positions of the barely visible subunits (α = 45 kDa, α' = 38 kDa, and β = 28 kDa) of CKII are marked (B, lane 2).

phosphorylation consensus sites for CKII, and upon their phosphorylation an additional 33 (22). Full phosphorylation of Nopp140, therefore, causes the enormous drop of its theoretical isoelectric point from extremely basic (10.3) to very acidic (4.1). To determine if Nopp140 was a substrate for CKII and if phosphorylation by CKII could account for the anomalous mobility of Nopp140 on SDS-PAGE, Nopp140 was expressed in bacteria and incubated in the absence (–) and presence (+) of purified sea star CKII (Fig. 1). When analyzed by SDS-PAGE, recombinant Nopp140 migrated with a M_r of 100 (Fig. 1, A and B, lanes 1). This mobility was slower than predicted from the calculated molecular mass of 73.6 kDa but was identical to the mobility of phosphatase-treated Nopp140 (not shown; Ref. 22). Upon incubation with CKII, Nopp140 was phosphorylated and showed the characteristic mobility shift from M_r 100 to M_r 140 (Fig. 1, A and B, lanes 2). As observed previously *in vivo* and in reticulocyte lysates *in vitro*, phosphorylation of recombinant Nopp140 by purified CKII also proceeded in an all-or-none fashion with only minor intermediate forms of phosphorylated Nopp140 present. Phosphorylation occurred equally well with ATP or GTP as phosphate source (not shown), a hallmark of phosphorylation by CKII. Taken together, these data indicate that phosphorylation alone accounts for the prominent mobility shift of Nopp140. Furthermore, the identical electrophoretic behavior of Nopp140 upon phosphorylation *in vivo* (22) and upon incubation by purified CKII *in vitro*, strongly incriminates CKII as the Nopp140 kinase *in vivo*.

The ability of CKII to phosphorylate Nopp140 to a high degree (Fig. 1; Ref. 22) supported our previous hypothesis that Nopp140 is identical to the mouse nucleolar protein pp135 (38), which was experimentally demonstrated to incorporate 75 phosphate groups per molecule upon incubation with CKII (45). To test this hypothesis directly, anti-pp135 antiserum (38) was obtained and used to probe Western blots of recombinant rat Nopp140. These antibodies recognized the bacterially expressed Nopp140 (not shown), thus confirming the identity of the two proteins.

The *in vitro* phosphorylation experiments also revealed that the phosphorylated form stained more strongly with silver than the unphosphorylated one even though there was less of the

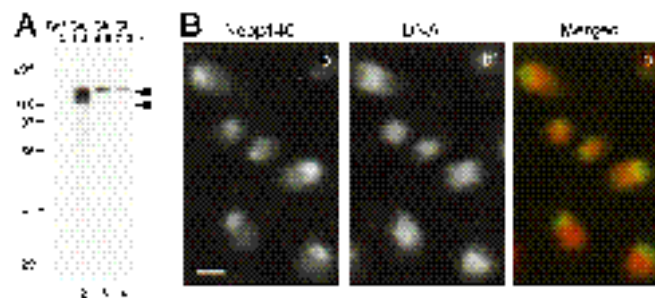


FIG. 2. Rat Nopp140 becomes fully phosphorylated (A) and is localized to the nucleolus (B) when expressed in yeast. Yeast cells (TMX12) carrying the rat Nopp140 cDNA under the inducible control of the *GAL10* promoter were analyzed by Western blotting (A) and indirect immunofluorescence (B) using anti-Nopp140 peptide antibodies. A, cells were grown in selective medium containing 2% raffinose (lane 1) followed by the induction of Nopp140 expression by switching to 2% galactose for 1.5 h (lane 2) and subsequent repression by growth in YPD for 3 h (lane 3) and 6 h (lane 4). The arrowheads mark the mobility of unphosphorylated and phosphorylated Nopp140. B, after growth for 1.5 h in the presence of 2% galactose, the cells were prepared for indirect immunofluorescence as described under "Experimental Procedures" and probed simultaneously for Nopp140 (b) and DNA (b') localization. B, b' shows the electronic superimposition of the Nopp140 (green) and DNA fluorescence (red) in false colors. Bar, 2 μ m.

phosphorylated form present when judged by Coomassie Blue staining (Fig. 1, compare B to A). This was not surprising, since silver stainability of nucleolar proteins has been previously correlated with their phosphoserine and phosphothreonine content (46). Nopp140, with its approximately 75 mol of phosphoserine, therefore, stained very strongly with silver (see Fig. 1B) and was further linked to pp135, which was characterized as one of the major silver-staining nucleolar proteins (47). The silver staining characteristic of Nopp140 is particularly noteworthy because it is the only such protein to date that is not only nucleolar but also present in coiled bodies (7) and, therefore, appears responsible for the silver-staining capacity of coiled bodies (48, 49).

Interestingly, bacterially expressed Nopp140 (Fig. 1, lane 1) and Nopp140 purified from rat liver nuclei (not shown) appeared also in dimeric and trimeric forms on SDS-PAGE as bands migrating at approximately 200 and 400 kDa (Fig. 1, lane 1, asterisks). The identity of these bands as Nopp140 dimer and trimer was confirmed by their reactivity with anti-Nopp140 antibodies on Western blots (not shown) and was indicated by their mobility shift upon CKII phosphorylation analogous to that of monomeric Nopp140 (Fig. 1B, lane 2) and by their ability to incorporate 32 P (see Fig. 8A, lane 4).

Phosphorylation and Localization of Rat Nopp140 in Yeast—Phosphorylation of Nopp140 was next studied in a heterologous system. Yeast contains CKII that is closely related to that of higher eukaryotes (50, 51) and that shows site specificity virtually identical to that of the rat liver enzyme (52). To determine, therefore, whether yeast was able to phosphorylate rat Nopp140 *in vivo*, the rat cDNA was placed under the control of the inducible *GAL10* promoter and transformed into yeast cells. Yeast cells were grown in selective medium containing 2% raffinose, the Nopp140 expression induced by switching to 2% galactose for 90 min, and further expression suppressed by subsequent growth in YPD. At various time points the expression of Nopp140 was monitored with anti-Nopp140 peptide antibodies (22) on Western blots of whole cell extracts (Fig. 2A). Rat Nopp140 was expressed in yeast and became phosphoryl-

ated as indicated by its characteristic mobility shift on SDS-PAGE (Fig. 2A, lane 2, arrowheads). During *de novo* synthesis of the rat Nopp140, *i.e.* in the presence of galactose (Fig. 2A, lane 2), intermediate forms of phosphorylated Nopp140 could also be detected, which were chased, however, into the fully phosphorylated form after Nopp140 expression was suppressed in glucose containing medium (Fig. 2A, lanes 3 and 4).

To localize the heterologously expressed Nopp140, indirect immunofluorescence was performed on fixed and permeabilized spheroplasts using the anti-Nopp140 peptide antibodies (Fig. 2B; Ref. 22). Rat Nopp140 localized predominantly to an area corresponding to one-third of the yeast nucleus (Fig. 2B, b), closely apposing the DNA stain (Fig. 2B, b') best visualized by the superimposition of the two images in false color (Fig. 2B, b'). This pattern was very characteristic of yeast nucleolar staining (see Fig. 6B). No labeling was observed prior to induction with galactose (not shown). Taken together these data demonstrated that yeast contained the kinase(s) necessary to phosphorylate and the cellular machinery to properly localize rat Nopp140 to the nucleolus.

Immunocross-reacting Species in Yeast Nucleoli—Antibodies raised previously against Nopp140 excised from SDS-PAGE gels (23) and against synthetic peptides of Nopp140 (22) did not cross-react with yeast proteins. To identify Nopp140 homologs in other species, a new antiserum was raised against the recombinant rat Nopp140 (see Figs. 1A, lane 1, and 8B, lane 2), which was available in large amounts. On Western blots this antiserum reacted with the recombinant Nopp140 (not shown) and with a single protein band of 140 kDa of rat liver nuclei (Fig. 3A, lane 1) and of whole BRL cell extracts (Fig. 3A, lane 2), demonstrating its specificity for Nopp140. In indirect immunofluorescence experiments on fixed and permeabilized BRL cells, this antiserum exhibited Nopp140-characteristic staining of the nucleolus and the coiled bodies (Fig. 3B; Refs. 7 and 23). When used to probe yeast cells, the anti-rat Nopp140 antiserum reacted with a crescent-shaped structure in yeast nuclei (Fig. 3, C and D). This structure was reminiscent of the yeast nucleolus in closely apposing the DNA stain (Fig. 3C'), particularly evident when the two images were superimposed in false colors (Fig. 3C'). Indeed, double immunofluorescence with antibodies against the bona fide yeast nucleolar antigen, Nop1 (40), revealed an identical pattern (Fig. 3, D and D'). When the two images were superimposed in false colors, *red* and *green*, the resulting *yellow-orange* color showed a perfect overlap of the two antigens (Fig. 3D'). Therefore, the anti-rat Nopp140 antibodies clearly cross-reacted with a yeast nucleolar antigen, possibly a Nopp140 homolog.

SRP40 Is Structurally and Immunologically Related to Nopp140—Nopp140 consists of three domains, the unique amino and carboxyl termini separated by the signature central domain of acidic serine clusters that alternate with exclusively basic stretches (Fig. 4A; Ref. 22). This overall structure is conserved among the rat (22), human (53–55), and *Xenopus* (42) Nopp140 homologs, as shown schematically in Fig. 4A. While the central domain is structurally conserved, the amino and carboxyl termini are conserved on an amino acid level, with the last 51 residues being most highly conserved and exhibiting 81% sequence identity between rat and frog (Fig. 4A). GenBank™ searches after deposition of the entire yeast genomic sequence with this conserved carboxyl terminus identified a single homologous yeast gene, *SRP40* (24), which corresponds to the open reading frame *YKR12* (56), and also expressed sequence tags from nematode (*Caenorhabditis elegans*) and plant (*Arabidopsis thaliana*). The alignment of the carboxyl termini of all related proteins, including the translations of the expressed sequence tags, is depicted in Fig. 4B. Analysis of this

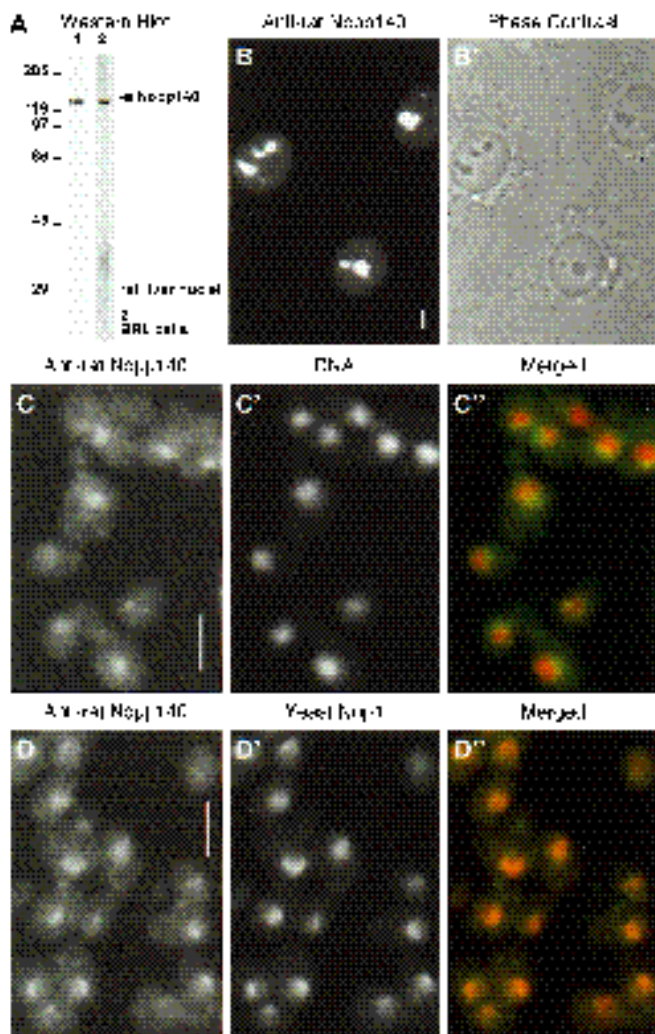


FIG. 3. Antibodies against the recombinant Nopp140 are specific for Nopp140 in rat cells (A and B) and cross-react with the yeast nucleolus (C and D). A, Western blots of rat liver nuclei (lane 1) and whole BRL cell lysates (lane 2) probed with the anti-Nopp140 antiserum. B, indirect immunofluorescence of the anti-Nopp140 antiserum on fixed and permeabilized BRL cells and the corresponding phase contrast picture (B'). Note the nucleolar and coiled body (extranucleolar dots) labeling. C, indirect immunofluorescence of the anti-Nopp140 antiserum on yeast spheroplasts probed simultaneously for DNA (C'). C', electronically merged image of the anti-Nopp140 (green) and DNA fluorescence (red) in false colors. D, indirect double immunofluorescence with anti-Nopp140 antiserum (D) and monoclonal antibodies against the nucleolar yeast Nop1 (D'). D', electronically merged image of the anti-Nopp140 (green) and anti-Nop1 (red) fluorescence in false colors. Note the perfect overlap indicated by the yellow-orange color. Bars, 5 μ m.

conserved Nopp140 tail for protein motifs revealed a consensus site for cAMP-dependent protein kinase that was conserved across all species (Fig. 4B, asterisk), suggesting a common sensory function of the carboxyl terminus for cAMP-mediated signals. SRP40 encodes a serine-rich protein of 41 kDa, SRP40, consisting of 48% serine residues that are mostly clustered in two long acidic stretches (Fig. 4C) containing 52 CKII consensus sites. In addition to these acidic serine stretches, which show structural resemblance to the acidic serine clusters of Nopp140, the carboxyl-terminal 51 amino acids of SRP40 exhibit 59% sequence identity to Nopp140 (Fig. 4C, boxed). Furthermore, SRP40 contains two minimal nuclear localization signal sequences, one SV40 large T antigen type sequence (57) and one bipartite sequence (Fig. 4C, underlined; Ref. 58).

To determine whether the anti-rat Nopp140 antibodies that

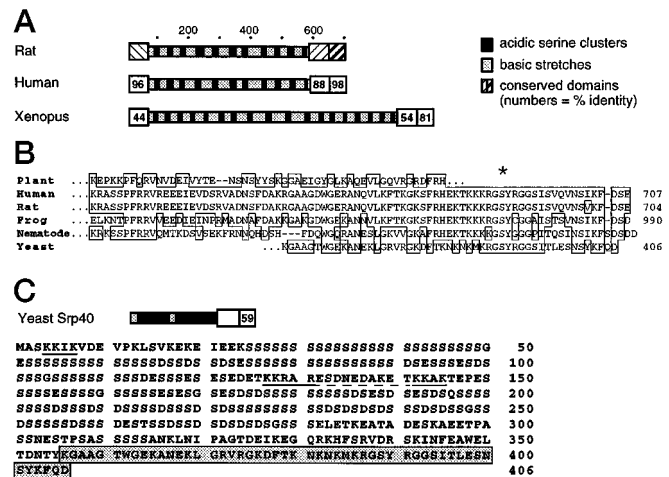


FIG. 4. Homologs of Nopp140. A, schematic alignment of rat Nopp140 (22) and its human (53, 54) and *Xenopus* (42) homologs drawn to scale. Black boxes indicate acidic serine stretches containing exclusively serines and glutamic and aspartic acid residues; gray boxes show exclusively basic stretches rich in lysine, alanine, and proline residues; striped boxes point out domains of sequence similarity with the numbers reflecting the percentage identity to rat Nopp140. The dots above the alignment indicate the numbers of residues with an increment of 100. B, amino acid sequence alignment of Nopp140 carboxyl termini from different species. Identical residues are boxed, but note, in addition, the many conservative changes. The asterisk indicates a conserved serine residue that constitutes a consensus site for cAMP-dependent protein kinase phosphorylation. The plant and nematode sequences were translated and assembled from expressed sequence tags with the accession numbers Z26471 (*A. thaliana*) and D36503, D27732, D32928, and D33633 (*C. elegans*). Note that all the sequences, despite considerable differences in overall length (see numbers, where available, on the left), end within three residues. C, schematic and amino acid sequence representation of the yeast SRP40 (24). The legend for the graphic depiction is as in A. The boxed and shaded residues highlight the conserved carboxyl terminus, and the underlined residues indicate minimal nuclear localization signals.

cross-reacted with the yeast nucleolus (Fig. 3) were able to recognize SRP40, the SRP40 gene was isolated from yeast genomic DNA using PCR and employed to express GST-SRP40 fusion proteins in *Escherichia coli*. Surprisingly, when full-length SRP40 was fused to GST (GST-SRP40), the 69-kDa fusion protein migrated with a M_r of close to 110 (Fig. 5A, lane 2). This aberrant migration was caused by the SRP40 moiety of the fusion protein, because GST alone (not shown) or GST fused to the conserved carboxyl-terminal 51 amino acids of SRP40 (GST-SRP40C-term) migrated according to their predicted molecular weight (Fig. 5A, lane 3). Therefore, the expected mobility of SRP40 alone would correspond to approximately 80 kDa or twice its actual molecular weight, analogous to the situation with rat Nopp140 (22). This abnormal migration is most likely caused by the long acidic theoretical isoelectric point of 3.9, close to that of fully phosphorylated Nopp140.

When the fusion proteins were probed on Western blots with the anti-rat Nopp140 antibodies, only the full-length fusion protein (Fig. 5B, lane 2), but not the conserved carboxyl-terminal 51-amino acid fusion protein (Fig. 5B, lane 3), was recognized by the polyclonal antiserum. This showed the rat Nopp140 and the yeast SRP40 to be immunologically related, apparently, through their acidic serine stretches and not their conserved carboxyl termini.

SRP40 Is a Nucleolar Protein—Because acidic serine clusters are also present in other yeast nucleolar proteins, such as NSR1 (14), it could not be established whether the yeast nucleolar signal observed with the anti-rat Nopp140 antibodies (Fig. 3) was due solely to cross-reactivity with SRP40. To de-

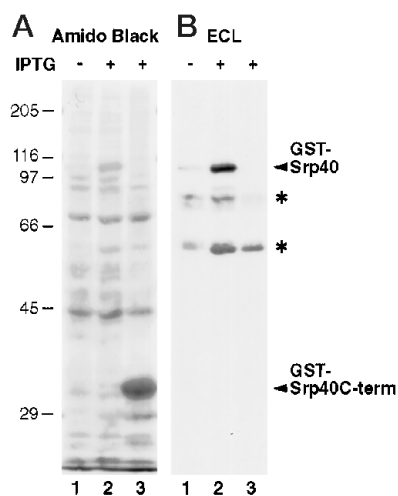


FIG. 5. Antirecombinant rat Nopp140 antibodies recognize bacterially expressed GST-SRP40 fusion protein on Western blots. Whole bacterial lysates, before (lanes 1) and after (lanes 2 and 3) the induction by isopropyl-1-thio- β -D-galactopyranoside of SRP40 expression as GST-fusion protein, either full-length (GST-SRP40, lanes 1 and 2) or the conserved carboxyl terminus alone (GST-SRP40C-term, lanes 3), were analyzed by Amido Black stain (A) and antibody reactivity (B) after SDS-PAGE and transfer to nitrocellulose. The antirecombinant Nopp140 antiserum also cross-reacted with some bacterial proteins (asterisks), which was not surprising, since the antibodies were raised against bacterially expressed Nopp140.

termine the intracellular location of SRP40, therefore, its gene was tagged with either a single amino or a double carboxyl-terminal HA-epitope, placed behind the inducible *GAL1* promoter, and expressed from a 2μ plasmid after transformation into a diploid wild type strain. Indirect immunofluorescence with anti-HA antibodies on cells grown overnight in selective medium containing 2% galactose showed that the HA-tagged SRP40 was expressed at different levels in various cells. The epitope-tagged protein did, however, localize consistently to a crescent-shaped structure closely apposing the DNA stain in a manner that is typical for the yeast nucleolus (Fig. 6A). This staining pattern was indistinguishable from that obtained with monoclonal antibodies against the yeast nucleolar marker antigen Nop1 (Fig. 6B; Ref. 40). In control experiments, no staining was observed with the anti-HA antibodies on cells that were treated identically but had been transformed with the vector alone (not shown). These results demonstrated that the epitope-tagged SRP40 was localized to the nucleolus and suggested an identical distribution for the endogenous SRP40.

To verify that the fluorescence pattern observed with the anti-HA antibodies corresponded to the full-length SRP40 and not to a breakdown product, total cell extracts were prepared and analyzed by SDS-PAGE, transferred to nitrocellulose, and visualized by Amido Black staining and by ECL after probing with anti-HA antibodies (Fig. 6C). As done for indirect immunofluorescence, cells transformed with the 2μ expression vector alone (Fig. 6C, lanes 2) or containing the HA-tagged SRP40 (Fig. 6C, lanes 1), were grown overnight in selective medium containing 2% galactose. The HA-tagged SRP40 was detected on Western blots as a single band migrating at a M_r of 80 (Fig. 6C, ECL lane 1, arrowhead) or at about twice its actual molecular weight, like the bacterially expressed protein (see Fig. 5), indicating a lack of major posttranslational modifications. The nucleolar localization and the abnormal migration of the HA-tagged SRP40 were independent of the location of the epitope, whether amino (not shown) or carboxyl-terminal (Fig. 6).

The SRP40 Gene Affects Cell Growth—To learn more about the function of SRP40, its gene and flanking regions were isolated from genomic DNA using PCR, and a construct was

created in which its open reading frame was replaced by the *URA3* marker gene (Fig. 7A). The insertion of this construct into the genome of two different diploid yeast strains, W303 and DF5, and the subsequent sporulation and tetrad dissection resulted in four viable spores in all cases after 2 days of growth at 30 °C (Fig. 7, B and C, *YPD*). Replica plating of the spores onto SC medium lacking uracil revealed the expected 2:2 segregation of the spores with and without integrated *URA3* gene representing the *srp40* Δ ::*URA3* and *SRP40* strains, respectively (Fig. 7, B and C, *SC-URA*). Proper integration of the *URA3* construct at the *SRP40* locus was confirmed by PCR on genomic DNA prepared from colonies of the different spores (not shown). Close inspection of the colonies showed that all the *srp40* Δ ::*URA3* colonies were about one-half of the size of the wild type colonies, as exemplified by the magnification of one of the tetrads (Fig. 7D). The adverse effect of *SRP40* gene deletion on cell growth was also observed in liquid culture (Fig. 7E). The following comparisons of *srp40* Δ ::*URA3* and wild type strains did not reveal any difference aside from the described growth defect. The analysis of the nucleolus using indirect immunofluorescence with the nucleolar marker Nop1 (40) showed that the integrity of the nucleolus remained unaffected (not shown). Furthermore, no accumulation of cells in a particular phase of the cell cycle was observed as judged by morphological comparison of two cultures (not shown).

Interestingly, while *SRP40* deletion led to only a minor growth impairment, its overexpression resulted in a severe growth defect (Fig. 7F), consistent with the previous identification of *SRP40* by a genetic screen for genes that cause growth arrest when overexpressed (26). Taken together, these data demonstrated that a specific level of *SRP40* gene expression was critical for optimal cell growth.

SRP40 Is a Weak Substrate for Casein Kinase II—Since SRP40 contained 52 consensus sites for CKII, three more than Nopp140, the recombinant GST-SRP40 fusion protein was subjected to a CKII phosphorylation assay identical to that employed for recombinant Nopp140 (see Fig. 1). Again sea star CKII was used because it phosphorylated Nopp140 to an identical degree as the rat liver enzyme, which exhibits the same site specificity as the yeast enzyme (52). As expected from the comparison of the mobility of the GST-SRP40 fusion protein and of the HA-tagged SRP40 expressed in yeast (see above; Figs. 5 and 6C), no slower migrating band on SDS-PAGE was observed upon CKII incubation of GST-SRP40, even after overdevelopment of the silver stain (not shown). However, when the incubation was performed using [γ - 32 P] ATP as phosphate donor, GST-SRP40 incorporated 32 P (Fig. 8A, lane 2). Therefore, GST-SRP40 was phosphorylated by CKII, however to a much lesser degree than equivalent amounts of Nopp140 (Fig. 8A, compare lanes 2 and 4) and without the dramatic mobility shift (Fig. 8, lane 4) observed with Nopp140 (Fig. 8, compare lane 4A with 2B). The lack of any trace of phosphorylation in the absence of CKII but presence of GTP and ATP or [γ - 32 P] ATP (Fig. 8A, lanes 1 and 3) demonstrated that neither Nopp140 nor GST-SRP40 underwent autophosphorylation.

DISCUSSION

This study reveals the yeast *SRP40* gene product, SRP40, as the structural and immunologically related homolog of the rat nucleolar phosphoprotein Nopp140. Nopp140 together with its partner NAP57 has been proposed to function as a chaperone in the nuclear transport of nucleolar components and/or ribosome assembly (7, 22). Such a chaperone function is also indicated for SRP40 in yeast by the requirement for a specific level of *SRP40* expression for optimal cell growth, as evidenced by the slow growth phenotype after both overexpression and deletion of *SRP40* (Fig. 7). This could be envisioned as follows. In the

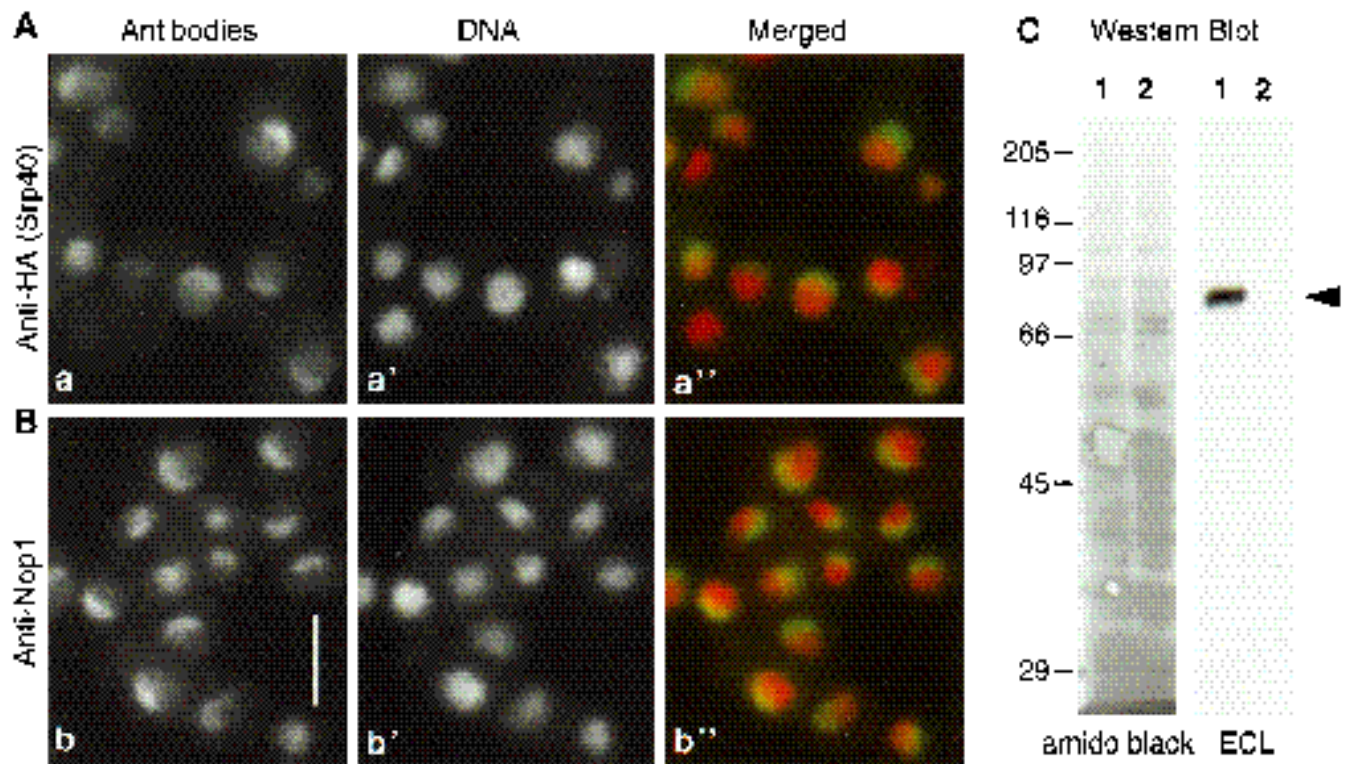


FIG. 6. SRP40 is a nucleolar protein. *A*, indirect immunofluorescence (see "Experimental Procedures") of HA-tagged SRP40 (*a*) expressed in yeast (TMX23) by growth in selective medium containing 2% galactose. The cells were counterstained for DNA (*a'*), and the two images superimposed in false colors (*a''*; anti-HA antibodies in *green* and DNA in *red*). *B*, cells expressing SRP40-HA as in *A* were stained for the endogenous nucleolar protein Nop1 (*b*) and DNA (*b'*), and the two pictures superimposed in false colors (*b''*; Nop1 in *green* and DNA in *red*). Bar, 5 μ m. *C*, Western blot of whole yeast cells grown as in *A* either expressing SRP40-HA (TMX23, lanes 1) or carrying the vector alone (TMX19, lanes 2). The nitrocellulose was stained for protein with *Amido Black* (left panel) and subsequently probed for SRP40-HA (arrowhead) with anti-HA antibodies (right panel), which were visualized by ECL.

absence of SRP40, ribosome biogenesis continues, albeit at a slowed pace, due to partially overlapping functions of other nucleolar proteins with acidic stretches, such as NSR1 (14), NPI46/FPR3 (59, 60), and UBF1 (61). Overexpression of SRP40, however, titrates out certain ribosomal proteins, all of which are required in equimolar amounts for ribosome assembly and consequent cell growth.

SRP40 was previously identified in two separate genetic screens. It was first described as a weak multicopy suppressor of a temperature-sensitive mutation in one of the common subunits of RNA polymerase I and III, AC40 (24), and second as a multicopy suppressor of a thermosensitive mutation in transcription factor IIIC (25). Since SRP40 localizes to the same subcellular compartment as RNA polymerase I, a physical interaction could occur between these two proteins. A direct interaction between SRP40 and RNA polymerase III or transcription factor IIIC, however, is more difficult to explain. One possible explanation for both phenotypes is that the dramatically reduced growth rate caused by *SRP40* overexpression (Fig. 7*F*; Ref. 26) allows the mutant RNA polymerases I and III and transcription factor IIIC to keep up with their functions well enough for slow cell growth to occur, reflecting an indirect and pleiotropic effect.

Based on the following observations, yeast SRP40 is the bona fide homolog of rat Nopp140. First, analysis of the primary sequence shows the two proteins contain at least two distinct domains that are conserved across evolution: the highly conserved carboxyl terminus, also present in nematode- and plant-expressed sequence tags (see Fig. 4*B*), and the acidic serine stretches, also found in mammalian nucleolin (13), budding yeast NSR1 (14), fission yeast GAR2 (62), and plant Rab17 (63, 64). Second, Nopp140 and SRP40 are immunologically related

as demonstrated by the cross-reactivity of the antibodies raised against the rat protein with the yeast protein. Third, SRP40, like Nopp140, is predominantly located in the nucleolus as judged by immunolocalization of the epitope-tagged protein. Fourth, the proposed function of Nopp140 as a chaperone in ribosome biogenesis is compatible with the phenotype of both *SRP40* gene deletion and overexpression. In fact, when rat Nopp140 was overexpressed in yeast it caused growth impairment like overexpression of SRP40, even though less pronounced (not shown).

While Nopp140 and SRP40 are similar in many ways, they also differ. In particular, Nopp140 is more highly phosphorylated by CKII than SRP40 leading to the dramatic drop of its theoretical isoelectric point of over 6 units from 10.3 to 4.1. These numbers closely match those of the larger *Xenopus* Nopp140 homolog (42), namely 10.4 and 4.0, the latter being in good agreement with the experimentally determined isoelectric point of 4.2 (43), thereby validating the theoretical values. Yeast SRP40, however, possesses an acidic isoelectric point of 3.9 even in the absence of phosphorylation. This makes it already one of the more acidic proteins in the cell and may explain why CKII barely introduces any further negative charges despite its 52 phosphorylation consensus sites. We previously showed that phosphorylation of rat Nopp140 was required for binding of basic nuclear localization signal peptides, demonstrating a potential regulatory role for phosphorylation *in vivo* (22). In contrast, the yeast Nopp140 homolog appears to be a constitutively acidic protein lacking the additional level of regulation found in its vertebrate counterparts.

Further information on the function of the two proteins can be gained from another difference. While yeast SRP40 lacks any consensus sites for Cdc2 kinase phosphorylation, Nopp140

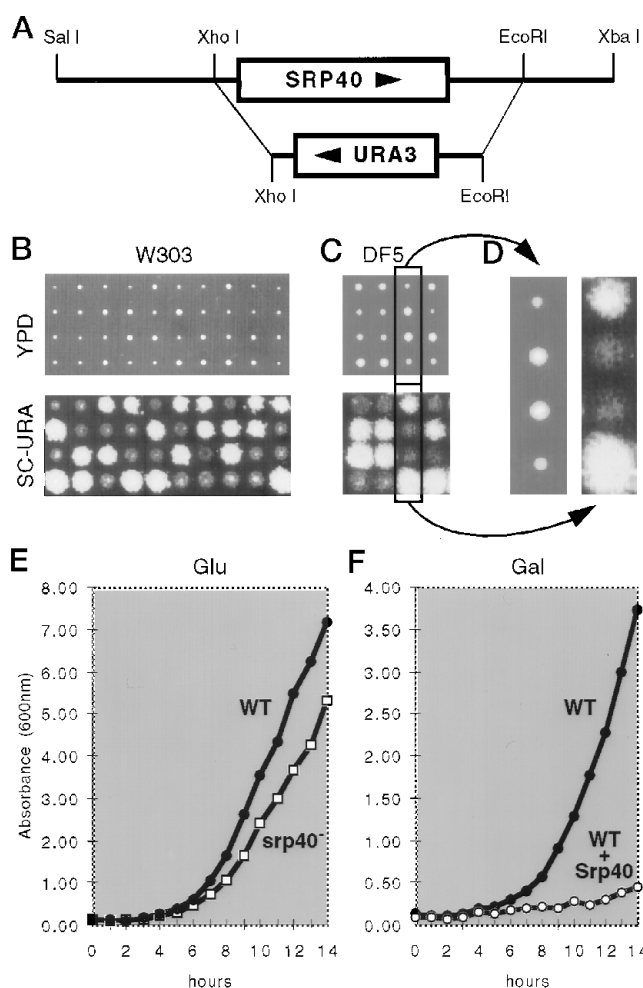


FIG. 7. Effects of *SRP40* gene deletion and overexpression on cell growth. *A*, schematic representation of the amplified *SRP40* gene including flanking sequences (3.2 kilobases) drawn to scale. The insertion sites of the *URA3* gene in reverse orientation are indicated. *B* and *C*, tetrad dissections of the diploid strains W303 (TMX14) and DF5 (TMX15) with one deleted copy of the *SRP40* gene (*srp40* Δ ::*URA3*). The alignment of 10 (*B*) and 4 (*C*) tetrads of haploid spores derived from W303 (*B*) or DF5 (*C*) is depicted grown on rich medium (YPD) for 2 days at 30 °C or replica-plated on SC medium lacking uracil (*SC-URA*). *D*, the enlargement of one tetrad from (*C*); note the co-segregation of the smaller colonies grown on YPD (*left*) with the uracil marker (*right*). *E*, growth curve of haploid wild type (*WT*, closed circles, F1104) and *SRP40*-deleted strain (*srp40* $^{-}$, open squares, TMY20) in SC medium containing 2% glucose. The cells were grown to late stationary phase and then diluted approximately 100-fold, and growth at 30 °C was determined by observing the absorbance at 600 nm. *F*, growth curve of a haploid wild type strain (*WT*, closed circles, F1104) and the same strain carrying *SRP40* under the inducible *GAL10* promoter (*WT* + *SRP40*, open circles, TMY28) in SC medium containing 2% galactose and, in the case of TMY28, lacking leucine. Growth in those media was determined as described for *E*.

contains 10, all of which are situated in the basic regions that separate the 10 acidic serine stretches (22). Insertion of negative charges by phosphorylation into those exclusively basic regions of Nopp140 could have dramatic structural consequences. Indeed, the human Nopp140 homolog has been demonstrated to become hyperphosphorylated during mitosis (53) concomitantly with the segregation of the nucleolus and the dispersion of Nopp140 (23, 53). Thus, Nopp140 is apparently phosphorylated by Cdc2 kinase during mitosis like two other vertebrate nucleolar proteins, nucleolin and NO38 (65, 66). In yeast, however, the nucleolus remains intact during mitosis (67, 68) and does not, therefore, require the phosphorylation and consequent dispersion of SRP40.

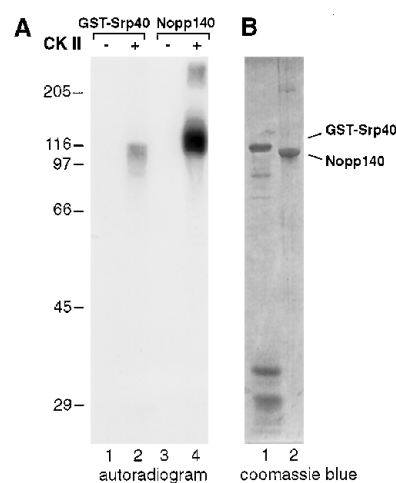


FIG. 8. CKII phosphorylates recombinant SRP40 to a much lesser extent than Nopp140. *A*, equal amounts of recombinant GST-SRP40 (*lanes 1* and *2*) and Nopp140 (*lanes 3* and *4*) were incubated with [γ - 32 P] ATP in the absence (*lanes 1* and *3*) and presence (*lanes 2* and *4*) of purified sea star CKII as described under "Experimental Procedures." The samples were subsequently analyzed by SDS-PAGE and autoradiography. *B*, recombinant GST-SRP40 (*lane 1*) and Nopp140 (*lane 2*) were analyzed by SDS-PAGE, side by side with the samples in *A*, and with Coomassie Blue stain to directly compare the mobility of the unphosphorylated (*B*) and phosphorylated (*A*) forms of the two proteins. Note that 4 times more protein was loaded in (*B*) than in *A*.

In summary, analysis of both the similarities and differences between Nopp140 and SRP40 points toward a common function in vertebrates and yeast. Thus, Nopp140 and SRP40 may serve as the glue or skeleton that holds the nucleolus together via ionic interactions between their negative charges and the basic ribosomal proteins. The observation of oligomeric forms (see Fig. 1) and tracks (22) of Nopp140 are particularly intriguing in this context. Having the yeast homolog of Nopp140 in hand now adds the possibility of a genetic approach to further define its function.

Acknowledgments—I am grateful to Alfred Anderer, John Aris, and Jonathan Backer for kind gifts of antibodies, to the Albert Einstein College of Medicine analytical imaging facility and Michael Cammer for use of and help with the confocal microscope, and to Wayne Grant for technical assistance. I greatly appreciate the help with yeast techniques by Amy Chang and Greg Prelich and, in particular, the critical support and comments throughout this study by Susan Smith. I thank Jon Warner and Mitch Bernstein for critical reading of the manuscript.

REFERENCES

- Traub, P., and Nomura, M. (1968) *Proc. Natl. Acad. Sci. U. S. A.* **59**, 777–784
- Shaw, P. J., and Jordan, E. G. (1995) *Annu. Rev. Cell Dev. Biol.* **11**, 93–121
- Prestayko, A. W., Klomp, G. R., Schmol, D. J., and Busch, H. (1974) *Biochemistry* **13**, 1945–1951
- Kumar, A., and Warner, J. R. (1972) *J. Mol. Biol.* **63**, 233–246
- Soeiro, R., and Basile, C. (1973) *J. Mol. Biol.* **79**, 507–519
- Jiang, W., Middleton, K., Yoon, H.-J., Fouquet, C., and Carbon, J. (1993) *Mol. Cell Biol.* **13**, 4884–4893
- Meier, U. T., and Blobel, G. (1994) *J. Cell Biol.* **127**, 1505–1514
- Ochs, R. L., Lischwe, M. A., Spohn, W. H., and Busch, H. (1985) *Biol. Cell* **54**, 123–134
- Aris, J. P., and Blobel, G. (1991) *Proc. Natl. Acad. Sci. U. S. A.* **88**, 931–935
- Jansen, R. P., Hurt, E. C., Kern, H., Lehtonen, H., Carmo-Fonseca, M., Lapeyre, B., and Tollervey, D. (1991) *J. Cell Biol.* **113**, 715–729
- Freeman, J. W., Busch, R. K., Gyorkey, F., Gyorkey, P., Ross, B. E., and Busch, H. (1988) *Cancer Res.* **48**, 1244–1251
- de Beus, E., Brockenbrough, J. S., Hong, B., and Aris, J. P. (1994) *J. Cell Biol.* **127**, 1799–1813
- Lapeyre, B., Bourbon, H., and Amalric, F. (1987) *Proc. Natl. Acad. Sci. U. S. A.* **84**, 1472–1476
- Lee, W.-C., Xue, Z., and Mélése, T. (1991) *J. Cell Biol.* **113**, 1–12
- Kondo, K., and Inouye, M. (1992) *J. Biol. Chem.* **267**, 16252–16258
- Xue, Z., Shan, X., Lapeyre, B., and Mélése, T. (1993) *Eur. J. Cell Biol.* **62**, 13–21
- Tollervey, D., Lehtonen, H., Jansen, R., Kern, H., and Hurt, E. C. (1993) *Cell* **72**, 443–457
- Girard, J.-P., Lehtonen, H., Caizergues-Ferrer, M., Amalric, F., Tollervey, D., and Lapeyre, B. (1992) *EMBO (Eur. Mol. Biol. Organ.) J.* **11**, 673–682

19. Jansen, R., Tollervey, D., and Hurt, E. C. (1993) *EMBO (Eur. Mol. Biol. Organ.) J.* **12**, 2549–2558
20. Sun, C., and Woolford Jr., J. L. (1994) *EMBO (Eur. Mol. Biol. Organ.) J.* **13**, 3127–3135
21. Bergès, T., Petfalski, E., Tollervey, D., and Hurt, E. C. (1994) *EMBO (Eur. Mol. Biol. Organ.) J.* **13**, 3136–3148
22. Meier, U. T., and Blobel, G. (1992) *Cell* **70**, 127–138
23. Meier, U. T., and Blobel, G. (1990) *J. Cell Biol.* **111**, 2235–2245
24. Lalo, D., Carles, C., Sentenac, A., and Thuriaux, P. (1993) *Proc. Natl. Acad. Sci. U. S. A.* **90**, 5524–5528
25. Lefebvre, O., Rùth, J., and Sentenac, A. (1994) *J. Biol. Chem.* **269**, 23374–23381
26. Espinet, C., De La Torre, M. A., Aldea, M., and Herrero, E. (1995) *Yeast* **11**, 25–32
27. Maniatis, T., Fritsch, E. F., and Sambrook, J. (1989) *Molecular Cloning: A Laboratory Manual* 2nd ed. Ed., Cold Spring Harbor Laboratory Press, Cold Spring Harbor, NY
28. Rosenberg, A. H., Lade, B. N., Chui, D., Lin, S., Dunn, J. J., and Studier, F. W. (1987) *Gene* **56**, 125–135
29. Smith, S., and Blobel, G. (1994) *Proc. Natl. Acad. Sci. U. S. A.* **91**, 10124–10128
30. Guan, K. L., and Dixon, J. E. (1991) *Anal. Biochem.* **192**, 262–267
31. Guarente, L., Yocum, R. R., and Gifford, P. (1982) *Proc. Natl. Acad. Sci. U. S. A.* **79**, 7410–7414
32. Wilson, I. A., Niman, H. L., Houghten, R. A., Cherenon, A. R., Connolly, M. R., and Lerner, R. A. (1984) *Cell* **37**, 767–778
33. Sikorski, R. S., and Hieter, P. (1989) *Genetics* **122**, 19–27
34. Gietz, D., St. Jean, A., Woods, R. A., and Schiestl, R. H. (1992) *Nucleic Acids Res.* **20**, 1425
35. Sherman, F., Fink, G. R., and Hicks, J. B. (1986) *Methods in Yeast Genetics*, Cold Spring Harbor Laboratory, Cold Spring Harbor, New York
36. Ausubel, F. A., Brent, R., Kingston, R. E., Moore, D. D., Seidman, J. G., Smith, J. A., and Struhl, K. (1993) *Current Protocols in Molecular Biology*, Greene Publishing and Wiley-Interscience, New York
37. Marston, F. A. O. (1987) in *DNA Cloning: A Practical Approach* (Glover, D. M., ed) Vol. 3, pp. 59, IRL Press, Oxford
38. Pfeifle, J., and Anderer, F. A. (1984) *Eur. J. Biochem.* **139**, 417–424
39. Pringle, J. R., Adams, A. E. M., Drubin, D. G., and Haarer, B. K. (1991) *Methods Enzymol.* **194**, 565–602
40. Aris, J., and Blobel, G. (1988) *J. Cell Biol.* **107**, 17–31
41. Fasman, G. D. (ed) (1978) *CRC Handbook of Biochemistry and Molecular Biology* 3rd Ed. Vol. 1. Proteins, CRC Press, Boca Raton, U. S. A.
42. Cairns, C., and McStay, B. (1995) *J. Cell Sci.* **108**, 3339–3347
43. Schmidt-Zachmann, M. S., Hügle, B., Scheer, U., and Franke, W. W. (1984) *Exp. Cell Res.* **153**, 327–346
44. Altschul, S. F., Gish, W., Miller, W., Myers, E. W., and Lipman, D. J. (1990) *J. Mol. Biol.* **215**, 403–410
45. Pfaff, M., and Anderer, F. A. (1988) *Biochim. Biophys. Acta* **969**, 100–109
46. Satoh, K., and Busch, H. (1981) *Cell Biol. Int. Rep.* **5**, 857–866
47. Pfeifle, J., Boller, K., and Anderer, F. A. (1986) *Exp. Cell Res.* **162**, 11–22
48. Lafarga, M., Hervás, J. P., Santa-Cruz, M. C., Villegas, J., and Crespo, D. (1983) *Anat. Embryol.* **166**, 19–30
49. Ramon y Cajal, S. (1910) *Trab. Lab. Invest. Biol. (Madrid)* **8**, 1–26
50. Chen-Wu, J. L.-P., Padmanabha, R., and Glover, C. V. C. (1988) *Mol. Cell Biol.* **8**, 4981–4990
51. Padmanabha, R., Chen-Wu, J. L.-P., Hanna, D. E., and Glover, C. V. C. (1990) *Mol. Cell Biol.* **10**, 4089–4099
52. Marin, O., Calderan, A., Ruzza, P., Borin, G., Meggio, F., Grankowski, N., and Marchiori, F. (1990) *Int. J. Peptide Protein Res.* **36**, 374–380
53. Pai, C.-Y., Chen, H.-K., Sheu, H.-L., and Yeh, N.-H. (1995) *J. Cell Sci.* **108**, 1911–1920
54. Nomura, N., Miyajima, N., Sazuka, T., Tanaka, A., Kawarabayasi, Y., Sato, S., Nagase, T., Seki, N., Ishikawa, K., and Tabata, S. (1994) *DNA Res.* **1**, 27–35
55. Nomura, N., Miyajima, N., Sazuka, T., Tanaka, A., Kawarabayasi, Y., Sato, S., Nagase, T., Seki, N., Ishikawa, K., and Tabata, S. (1994) *DNA Res.* **1**(Supplement), 47–56
56. Bou, G., Esteban, P. F., Baladron, V., Gonzalez, G. A., Cantalejo, J. G., Remacha, M., Jimenez, A., Del Rey, F., Ballesta, J. P. G., and Revuelta, J. L. (1993) *Yeast* **9**, 1349–1354
57. Chelsky, D., Ralph, R., and Jonak, G. (1989) *Mol. Cell Biol.* **9**, 2487–2492
58. Robbins, J., Dilworth, S. M., Laskey, R. A., and Dingwall, C. (1991) *Cell* **64**, 615–623
59. Benton, B. M., Zang, J.-H., and Thorner, J. (1994) *J. Cell Biol.* **127**, 623–639
60. Shan, X., Xue, Z., and Mélése, T. (1994) *J. Cell Biol.* **126**, 853–862
61. Jantzen, H.-M., Admon, A., Bell, S. P., and Tjian, R. (1990) *Nature* **344**, 830–836
62. Gulli, M.-P., Girard, J.-P., Zabetakis, D., Lapeyre, B., Mélése, T., and Caizergues-Ferrer, M. (1995) *Nucleic Acids Res.* **23**, 1912–1918
63. Goday, A., Jensen, A. B., Culiáñez-Macià, F. A., Albà, M. M., Figueras, M., Serratos, J., Torrent, M., and Pagès, M. (1994) *Plant Cell* **6**, 351–360
64. Vilardell, J., Goday, A., Freire, M. A., Torrent, M., Martínez, M. C., Torne, J. M., and Pagès, M. (1990) *Plant Mol. Biol.* **14**, 423–432
65. Belenguer, P., Caizergues-Ferrer, M., Labbé, J.-C., Dorée, M., and Amalric, F. (1990) *Mol. Cell Biol.* **10**, 3607–3618
66. Peter, M., Nakagawa, J., Dorée, M., Labbé, J. C., and Nigg, E. A. (1990) *Cell* **60**, 791–801
67. Granot, D., and Snyder, M. (1991) *Cell Motil. Cytoskelet.* **20**, 47–54
68. Robinow, C. F., and Marak, J. (1966) *J. Cell Biol.* **29**, 129–151